



Fermi National Accelerator Laboratory

FERMILAB-Pub-93/020-A
January 1993

The Phenomenological Status of Late Time Phase Transition Models after COBE *

Xiaochun Luo and David N. Schramm

University of Chicago

Astronomy and Astrophysics Center

5640 S. Ellis Ave., Chicago, IL 60637

and

NASA/Fermilab Astrophysics Center, Fermilab, Box 500, Batavia, IL 60510

ABSTRACT

Some relatively model independent results for structure formation via late time phase transitions (LTPT) are discussed. In particular, generic LTPT power spectra are presented. The implication of the recent COBE detection of the cosmic background radiation (CBR) anisotropy at large angular scales ($\gtrsim 7^\circ$) and the tight upper limits from small angular scales ($\sim 1^\circ$) to LTPT models are discussed. Special attention is focused on the observational constraints and possible non-Gaussian signatures of CBR temperature anisotropies from LTPT and other non-Gaussian models. It is shown that while LTPT have been seriously constrained by the recent data, viable models do remain which provide more power on the 100 – 200Mpc scales than do more traditional primordial Gaussian density fluctuation models. Tests for such models are presented, including possible anisotropies on angular scales < 8 arcminutes.

* Submitted to ApJ.



Introduction

One of the major questions in cosmology today is the origin of cosmic structure. Models for structure formation have been constrained tremendously by the recent measurements and limits placed on the anisotropy of the cosmic background radiation (CBR) by the COBE satellite (Smoot et al. 1992; Wright et al. 1992; Bennett et al. 1992) and by balloon experiments (Meyer et al. 1991) and studies at the South Pole (Gaier et al. 1992). These measurements from the recombination epoch are confronted by the traditional observations of the distributions of galaxies and clusters of galaxies on scales of 10's to 100's of Mpc. Models for structure formation generally consist of assumptions about composition (percentages of baryons and hot (HDM) and/or cold (CDM) non-baryonic dark matter) coupled with some assumptions about the seeds to initiate the clumping of the matter. Seeds can be divided into different categories. For example, Gaussian density fluctuations versus topological defects, or primordially generated versus possible generation after recombination. This latter category of late time generation of seeds (which could produce Gaussian and/or topological seeds) is the class of seeds we will focus on in this paper. Possible physical mechanisms for such late time seed generation include low temperature fundamental phase transitions (Hill, Schramm, & Fry 1989; Press, Ryden, & Spergel 1990; Frieman, Hill & Watkins 1992) or maybe even some instability at the end of recombination itself (Klemperer et al. 1992). We will refer to all such seed generation mechanisms as late time phase transitions (LTPT), although the recombination proposal is an instability rather than a true phase transition. The purpose of this paper is to examine the current status of LTPT in the light of the new observational data. In particular, we will address the issues of the viability of LTPT after COBE, and whether LTPT present any possible advantage over more conventional models (Gaussian density fluctuations). We will also discuss possible tests that will eventually confirm or decisively kill LTPT.

Before addressing these points, let us review a motivation behind LTPT which will guide our discussion. One of the key concepts of standard cosmology is the particle horizon. It sets the scale within which causal physics processes are important. The horizon size R is evolving as the universe expands. In the matter dominated epoch, $R = H_0^{-1} / \sqrt{(1+z)}$, where H_0 is the present Hubble constant and z is the redshift. It is interesting to note that the comoving horizon size at redshift $z \sim 100$ is approximately $300h^{-1}$ Mpc, which

is about the same size as the largest structure observed today (Geller & Huchra 1989; Bahcall 1992). This interesting relation is a prime motivation for us to pursue the possibility that the perturbation of large scale structures in the universe today is created at redshift $z \sim 100$. Since this epoch is after the recombination epoch, it falls in the generic domain of LTPT. This paper will discuss some relatively model independent results of LTPT, including the required shape of the implied power spectrum, the implication of the recent COBE detection of CBR anisotropies at large angular scales ($\gtrsim 7^\circ$) and the tight upper limits from small angular scales ($\sim 1^\circ$) to the model and the possible non-Gaussian signature of CBR anisotropies from LTPT and the observational limits.

(1) Power Spectra from LTPT

For discussion, let us set the phase transition epoch to be at $z \sim 100$, which corresponds to a comoving scale of $\lambda_c \sim 300h^{-1}\text{Mpc}$. The density perturbations inside the horizon are very model dependent, a point to which we will return later. However, it is straight forward to calculate the power spectrum on the superhorizon scale. It is just a white noise spectrum

$$P_0(k) \sim k^0, \quad (1.1)$$

since the density fluctuations are simply the incoherent sum over different horizon volumes. However, the equal time power spectrum should take into account the different growth factors that different wavelengths have. All the density waves whose wavelength is larger than this value are superhorizon and the amplitude of the perturbation will not grow until it is inside the horizon at some later epoch. Thus, the processed superhorizon power spectrum is:

$$P(k) = \left(\frac{a(\lambda)}{a(\lambda_c)}\right)^2 P_0(k). \quad (1.2)$$

It is convenient to express the comoving horizon λ and the evolution of the density perturbation δ as a function of the scale factor of the background metric $R(t)$ (Weinberg 1972; Kolb & Turner 1990):

$$\lambda(R) = \frac{1}{H_0} \int_0^R \frac{dx}{[x^2(1 - \Omega_m - \Omega_v) + \Omega_m x + \Omega_v x^4]^{1/2}} \quad (1.3)$$

and

$$\frac{d^2 \delta}{d^2 R} + \frac{1}{R} f(R) \frac{d\delta}{dR} - \frac{3\Omega_m}{2R^2} \delta = 0 \quad (1.4)$$

where Ω_m, Ω_v are the mass fraction of matter and vacuum at the present epoch and the function $f(R)$ is

$$f(R) = 2 + \frac{\Omega_v - \Omega_m/2R^3}{\Omega_v + \Omega_m/R^3 + (1 - \Omega_m - \Omega_v)/R^2}, \quad (1.5)$$

which is determined from the Friedman equation:

$$H^2 = \frac{\dot{R}^2}{R^2} = H_0^2 [\Omega_v + \Omega_m/R^3 + (1 - \Omega_m - \Omega_v)/R^2]. \quad (1.6)$$

We can parameterize the density evolution as: $\delta(R) = a(R)\delta_0$, where δ_0 is the perturbation generated at the phase transition epoch and $a(R)$ is the growth factor of the perturbation. To find the power spectrum, one has to relate $a(R)$ to the comoving wavelength λ , which can be done by inverting the function found in Eq.(1.3). The equations (1.3) and (1.4) are solved numerically and they are shown in Fig. (1) and (2) for three different cosmological models:

- (1) $\Omega = 1$ matter (either CDM and/or HDM) dominated universe,
- (2) $\Omega = \Omega_m = 0.2$, an open universe with matter density of 0.2.
- (3) $\Omega = 1, \Omega_m = 0.2, \Omega_v = 0.8$, a cosmological constant dominated case.

The familiar result $a(R) = R, \lambda \sim \sqrt{R}$ is obtained for case (1). The shape of the power spectrum on scale $\lambda > \lambda_c$ is

- (1) $P(k) \sim k^4$;
- (2) $P(k) \sim k^4$ on scale between $\lambda_c \sim 300\text{Mpc}$ and $\lambda_d \sim 1000\text{Mpc}$; on the larger scales, $P(k) \sim k^1$;
- (3) the situation is almost identical to case (2), which indicates that the shape of the spectrum is determined primarily by the matter content of the universe.

On the subhorizon scale, the large scale redshift surveys provide us with a fair amount of data on certain aspects of the required power spectrum. Thus, we can determine certain aspects of the required power spectrum of density perturbations empirically. Unlike primordial fluctuations, LTPT are still relatively unconstrained as to the specific nature of the spectrum of seeds generated. As noted by Hill et al. (1989), different models are able to produce a wide range of possibilities. Hence, empirically derived spectra are in fact quite acceptable and in some sense are the preferred LTPT spectra.

In previous papers (Luo & Schramm 1992a; Szalay & Schramm 1985), we have shown that the two point correlation function for galaxies, clusters, cD galaxies, X-rays galaxies, QSO's and the superclusters can be written in a scale invariant way:

$$C(r) = \beta(L)(r/L)^{-1.8}, \quad (1.7)$$

where L is the average distance between objects in the surveys and the dimensionless clustering amplitude is about 0.26, which indicates the underlying density field may be scale invariant up to $\sim \lambda_c$. A power spectrum derived from Eq. (1.7) of a scale invariant density field (fractal) will follow a power law with index $n = 1.8 - 3 = -1.2$, or

$$P(k) \sim k^{-1.2}, \quad (1.8)$$

on subhorizon scales. Thus, the overall shape of the power spectrum from LTPT can be approximated as the following:

$$(1) P(k) = \begin{cases} A(k/k_c)^4, & k \leq k_c; \\ A(k/k_c)^{-1.2}, & k \geq k_c. \end{cases} \text{ for } \Omega = 1 \text{ matter dominated universe.}$$

$$(2) \text{ or } (3): P(k) = \begin{cases} A(k_d/k_c)^3(k/k_c)^1, & k \leq k_d; \\ A(k/k_c)^4, & k_d \leq k \leq k_c, \text{ where } k_c = 2\pi/\lambda_c, k_d = 2\pi/\lambda_d. \\ A(k/k_c)^{-1.2}, & k \geq k_c. \end{cases}$$

The normalization of the power spectrum can be done by using the small scale galaxy correlations or by using the CBR quadruple moment on large scales. Similar to the well known CDM model, we can parameterize the normalization by a biasing factor b . The constraint on b can be obtained from the CBR anisotropy, which will be discussed in the next section.

(2) Normalization of the Power Spectrum

Before discussing the normalization of the power spectrum produced by LTPT, let us first review the technique used in the conventional CDM model. There are two options to normalize the spectrum: either by the galaxy-galaxy correlation function $\xi(r)$ on small scale or by the CBR quadrupole observed by COBE on large scale. The commonly used normalizations on small scale are (Davis & Peebles 1983; Dressler et al. 1987):

$$\frac{\Delta M}{M} |_{8h^{-1}\text{Mpc}} = 1; \quad (2.1)$$

$$J_3(10h^{-1}\text{Mpc}) = 270h^3 \text{Mpc}^3; \quad (2.2)$$

$$v_{rms}(50h^{-1}\text{Mpc}) = 500\text{km/s.} \quad (2.3)$$

On large scale, if the perturbations are primordial and the temperature fluctuation is due to the Sachs-Wolfe effect, then the quadrupole moment will be:

$$a_2^2 = \frac{AH_0^4}{16} \frac{1}{\Gamma(3/2)^2\Gamma(3)}, \quad (2.4)$$

for a scale invariant Harrison-Zeldovich ($n=1$) spectrum. The observed rms quadruple Q is

$$Q^2 = \{(2l+1)/4\pi\}a_2^2. \quad (2.5)$$

COBE's detection (Smoot et al. 1992; Wright, et al. 1992) of $Q = (4.8 \pm 1.5) \times 10^{-6}$ thus provides the normalization of the spectrum on large scale.

The observations on small scale come from high density peaks like galaxies and clusters, which are not the underlying density field. But the CBR fluctuation is probing the density field itself. One usually parametrizes the discrepancy by introducing a biasing parameter b , where $(\frac{\delta\rho}{\rho})_{mass} = \frac{1}{b}(\frac{\delta\rho}{\rho})_{light}$. COBE results suggest that such a constant biasing parameter is unity for the CDM model. However, such a normalization would then have a problem in understanding why the apparent Ω_m implied by galactic rotation curves is $\lesssim 0.1$. Primordial CDM models thus now tend to prefer a scale dependent bias or utilize mixtures of CDM with HDM (Schaefer & Shafi 1992; Davis, Summers, & Schlegel 1992; van Dalen & Schaefer 1992). In this paper, we will instead appeal to LTPT.

The normalization of the power spectrum for LTPT on large scale is slightly different than primordial cases since CBR fluctuations are related to the time changing gravitation potential through (Jaffe, Stebbins & Frieman 1992):

$$\left(\frac{\Delta T}{T}\right)_{LTPT} = 2 \int \dot{\Phi} d\eta, \quad (2.6)$$

rather than the potential Φ itself on the surface of last scattering (Sachs-Wolfe effect)

$$\left(\frac{\Delta T}{T}\right)_{SW} = \frac{1}{3}\Phi. \quad (2.7)$$

The temperature fluctuations are frequently written in terms of the temperature correlation function

$$C(\theta) = \langle \frac{\Delta T}{T}(\hat{m}) \frac{\Delta T}{T}(\hat{n}) \rangle = \frac{1}{4\pi} \sum (2l+1) C_l P_l(\hat{m} \cdot \hat{n}), \quad (2.8)$$

where the multipole amplitude for Sachs-Wolfe effect is:

$$C_l^{SW} = \frac{H_0^4}{8\pi^2} \int dk k^{-2} P(k) j_l(k\eta)^2, \quad (2.9)$$

and

$$C_l^{LTPT} = \frac{9H_0^4}{2\pi^2} \int dk k^{-2} P(k) \left| \int_{\eta_0}^{\eta} d\eta j_l(k(\eta_0 - \eta)) \dot{f}_k(\eta) \right|^2. \quad (2.10)$$

In the model when the density perturbation is produced by a phase transition at redshift $z \sim 100$, in the large scale limit, $k \rightarrow 0$

$$C_l^{LTPT} \rightarrow 36C_l^{SW}, \quad (2.11)$$

which is independent of l and the wavelength.

When we normalize the power spectra from LTPT by the COBE detected quadruple, the power on the scale to which COBE is sensitive will be 36 times smaller than that from a primordial spectrum. In terms of a biasing parameter, for the three cases we studied in the previous section, the constraints are:

(i) The power spectrum of $\Omega = 1$ matter dominated universe is shown in Fig. 3. If we normalize the density field to COBE, one finds that on small scales the density field should be anti-biased and the biasing parameter should be about $b \approx 1/8$ to fit the observations. If we normalize the power to small scale and assume that the biasing factor is $b=1$, the observed CBR temperature anisotropy will be lower than the COBE level by two orders of magnitude. This pure LTPT model is basically ruled out by COBE's detection of CBR temperature fluctuations at the level of 10^{-5} unless one is willing to accept antibiasing and allow a power law index $n \sim 4$ rather than the COBE observed $n = 1.1 \pm 0.6$ on large scale. However, mixed models where primordial fluctuations generate CBR fluctuations on large scale and LTPT generate small scale structure are still viable and we will discuss them later.

(ii) The power spectrum for an open universe or cosmological constant Λ dominated universe with $\Omega_m = 0.2$ is shown in Fig. 4. This LTPT model does fit the observations including the extra power observed by the APM survey. The biasing parameter is about 1 for these models and the effective power law index of the power spectrum is also within the COBE limits. But the models suffer the theoretical flaw of being "unnatural" in the sense that inflation and the flatness problem itself argue for a flat universe and Λ dominated models require a precise tuning of Λ to 121 decimal places (Carroll, Press, & Turner 1992).

(3) HDM with LTPT models

The previous section discussed the case where LTPT was solely responsible for the density perturbations observed today. However, it is still plausible that primordial density perturbations produce the large angular CBR fluctuations while LTPT dominate the small scale perturbations. In this mixed case, if the matter content of the universe is cold dark matter, it will do more harm than good, since the power on small scale predicted by the unbiased CDM model is already too high. However, if the dark matter candidate is a light massive neutrino, the small scale power generated by LTPT solves the problems of traditional HDM models where small scale power is erased by neutrino free streaming. The power spectrum of the mixed case, normalized to COBE on large scale and $\frac{\delta\rho}{\rho} = 1$ at $8h^{-1}\text{Mpc}$ (choose the biasing factor $b=1$) is shown in Fig. (4). The characteristic feature of the power spectrum is that there is a power enhancement at the scale which corresponds to the comoving horizon size of the LTPT epoch.

The arguments can be made quantitative by comparing the angular two point correlation $\omega(\theta)$ predicted from the model described above with the observations from the APM survey. The angular correlation function $\omega(\theta)$ is related to the spatial two point correlation function $\xi(r)$ through Limber's equation (Peebles, 1980):

$$\omega(\theta) = E^{-2} \int_0^\infty (y_1 y_2)^2 dy_1 dy_2 \phi(y_1) \phi(y_2) \xi(r), \quad (3.1)$$

where $r = D(y_1^2 + y_2^2 - 2y_1 y_2 \cos(\theta))^{1/2}$, $E = \int_0^\infty y^2 \phi(y) dy$ and ϕ is the selection function. We adopt the following selection function in accordance with the APM survey (Peacock 1991; Kashlinsky, 1992):

$$\phi(y) \approx y^{-0.5} e^{-(y/D)^2}. \quad (3.2)$$

The characteristic scale D is chosen to be $232h^{-1}\text{Mpc}$ as used by Peacock (1991) for the APM survey. As shown in Fig. (6), HDM with an LTPT predicts an angular two point correlation function that fits the APM observations remarkably well. In contrast, the standard CDM model predicts an angular two point function which falls off too rapidly on larger ($> 1^\circ$) angular scales. It is easy to understand physically why primordial models fail to fit the APM data while LTPT models naturally accommodate it. If the perturbation is generated primordially, it will not grow until the universe is matter dominated. Thus, the horizon size at the matter-radiation equality epoch, $\lambda_{EQ} \sim 13(\Omega h^2)^{-1}\text{Mpc}$, which sets the

correlation scale of the density perturbation, is just too small compared to the characteristic correlation scale implied by the APM data. On the other hand, the correlation length scale in LTPT is the horizon size at the epoch of LTPT, which is fairly large. Thus, more power on large scale is allowed thus fitting the APM data.

One concern regarding the power enhancement at the intermediate scale is the tight bound from the CBR measurement on these scales. This situation will be addressed in the next section.

(4) Small Scale ($< 3^\circ$) CBR Fluctuations

Before we get into the discussion of small scale angular anisotropy, let us discuss first the beam smearing effect: all experiments are done with finite beam width σ and the beam can be well approximated as a Gaussian:

$$f(|\hat{m} - \hat{n}|, \sigma) = \frac{1}{2\pi\sigma^2} e^{-|\hat{m} - \hat{n}|^2/2\sigma^2}, \quad (4.1)$$

and the observed temperature correlation function will be the convolution of the theoretical correlation (infinite thin beam) with the beam (Wilson & Silk 1981; Gouda, Sasaki, & Suto; 1989), which is

$$C(|\hat{m} - \hat{n}|, \sigma) = \int d\Omega'_1 d\Omega'_2 f(|\hat{m} - \hat{m}'|, \sigma) f(|\hat{n} - \hat{n}'|, \sigma) C(|\hat{m}' - \hat{n}'|, 0). \quad (4.2)$$

The multipole expansion of the correlation function is:

$$C(|\hat{m} - \hat{n}|, 0) = \sum_l (2l + 1) C_l(0) P_l(\hat{m}\hat{n}), \quad (4.3)$$

then the observed correlation is

$$C(|\hat{m} - \hat{n}|, \sigma) = \sum_l a_l(\sigma) (2l + 1) C_l(0) P_l(\hat{m}\hat{n}), \quad (4.4)$$

where $a_l(\sigma) = |j_l(i/\sigma^2)|^2$ which is just the l -th order spherical Bessel function of imaginary argument. In the limit of small σ , the formula reduces to

$$a_l(\sigma) = e^{-(l+0.5)^2\sigma^2}, \quad (4.5)$$

which is the commonly adopted formula.

By combining COBE and the power spectrum suggested by APM, if the density perturbation is generated primordially, the predicted small angle temperature anisotropy is (Kashlinsky 1992):

$$\left(\frac{\delta T}{T}\right)_{\theta=1.5^\circ} \approx 1.3 \times \left(\frac{\delta T}{T}\right)_{\text{COBE}} \approx 1.4 \times 10^{-5}, \text{ and } \left(\frac{\delta T}{T}\right)_{\theta=3.8^\circ} \approx 1.2 \times \left(\frac{\delta T}{T}\right)_{\text{COBE}} \approx 1.3 \times 10^{-5}, \quad (4.6)$$

The small scale CBR anisotropy depends on the details of how the gravitational potential is generated, thus a wide variety of values are allowed. As shown by Jaffe, Stebbins, & Frieman (1992), the minimal small scale temperature fluctuation in LTPT models is reduced by a factor of $\left(\frac{36}{k\eta_0}\right)$,

$$\left(\frac{\delta T}{T}\right)_{\text{LTPT}}^\theta \sim \left(\frac{\theta}{\theta_0}\right) \left(\frac{\delta T}{T}\right)_{\text{Primordial}}^\theta, \quad (4.7)$$

where $\theta_0 \approx 3^\circ$. Thus the predictions from LTPT for the UCSB South Pole and MIT balloon experiments will be 7×10^{-6} and 1.4×10^{-5} respectively. Furthermore, $\delta T/T$ decreases linearly with the decrease of the angular scale which the experiment probes. These results are consistent with the tight limit from the UCSB South Pole experiments (Gaier et al. 1992). However, the predicted minimal $\delta T/T$ is far below the recent detection of MAX (Meinhold et al. 1992) of several times 10^{-5} at the 0.5° scale.

For the mixed HDM and LTPT models, $\delta T/T$ is a sum of the contribution from both primordial and LTPT processes. Since the contribution from LTPT at small scale is small compared to primordial perturbations, the result will be about the same as the values given by Eq. (4.6).

If the density perturbations are generated primordially, the CBR anisotropy on the arcminute scales will be smoothed due to the finite thickness of the last scattering surface (Kolb & Turner 1990) and Silk damping (Silk 1967). However, smoothing effects will not occur in LTPT. The precise amplitude of $\frac{\delta T}{T}$ on arcminute scales depends on the detailed model of LTPT, but, in general, it will be the same order of magnitude as on degree scales, which $\sim 10^{-5}$. Thus, a detection of anisotropy on arcminute scales provides a positive test of LTPT models.

(5) Tests of Non-Gaussian Temperature Fluctuations on Small Scales

The reported large scale ($\theta \gtrsim 10^\circ$) cosmic microwave background radiation (CBR) anisotropy (Smoot et al. 1992; Wright et al. 1992) of COBE and its subsequent verification

(Ganga et al. 1993) constrains all models of cosmic structure formation. Models which assume a flat, Harrison-Zeldovich spectrum and random phase, Gaussian fluctuations have been the easiest to calculate and the most widely discussed. Such models are also a natural consequence of the inflation scenario (Bardeen, Steinhardt, & Turner 1983; Guth & Pi 1982; Hawking 1982; Starobinskii 1982). When these fluctuation models are used with pure cold dark matter (CDM) and normalized to the COBE anisotropy they appear to be in conflict with galaxy velocity dispersions at ~ 10 Mpc and are at most marginally consistent (Gorski 1992) with limits on $\Delta T/T$ at the one degree scale, the UCSB experiment at 1.2 degrees (Gaier et al. 1992): $\delta T/T < 1.4 \times 10^{-5}$, and the MIT balloon experiment (Meyer et al. 1991) at 3.8 degrees: $\frac{\delta T}{T}_{3.8^\circ} < 1.6 \times 10^{-5}$. Kashlinsky (1992) showed that the combination of the COBE and APM redshift surveys with Gaussian assumptions will give rise to a minimum temperature anisotropy $\frac{\delta T}{T} \sim 1.5 \times 10^{-5}$ on the one degree angular scale, corresponding to a sky signal of $40 \mu K$, which is in conflict with the 95% C.L. limits of the UCSB results. Gorski (1992) also showed that the tight bound on small scales may be in conflict with the large scale velocity flows.

Obviously, the final word on the anisotropies and the velocity flow data has not been written yet and future data may be able to fit this standard CDM model. It has also been shown that modifications of the model can be made to work which still retain the Gaussian-random-phase nature of the fluctuations, for example, a spectrum tilted with respect to the flat Harrison-Zeldovich spectrum (Freese, Frieman & Olinto 1991) or maybe a mix of hot-dark matter (HDM) along with CDM (Schaefer & Shafi 1992; Davis, Summers, & Schlegel 1992; van Dalen & Schaefer 1992) or maybe just a biasing factor that is scale-length dependent. However, in this section, we address the assumption of a non-Gaussian distribution as the variation to resolve potential difficulties.

As mentioned earlier, non-Gaussian temperature fluctuations occur in theories where cosmic structure is generated by topological seeds which are left over from a vacuum phase transition. Non-Gaussian temperature fluctuations can arise at various angular scales: the collapsing of a texture (Turok & Spergel 1991) at moderate redshift (\sim few) will give rise to hot and cold spots on the CBR sky at a large angular scale; the collapsing of subhorizon-sized vacuum bubbles (Gortz 1991, Turner, Watkins, & Widrow 1991) from a late-time phase transition (Hill, Schramm, & Fry, 1989) ($z \sim 100$) will also produce

hot and cold spots but on one degree scales; cosmic strings will give rise to temperature fluctuations at even smaller scales (\sim arcminutes). Therefore, the Gaussianity of the distribution of CBR temperature anisotropy provides a definite test of the possible scenario to generate cosmic structure. The Gaussianity tests we discuss here apply to LTPT and other topological seeds. Remember in general, LTPT can produce all sorts of topological seeds (Hill, Schramm, & Widrow 1990) whereas plausible primordial defects tend to be strings and textures.

In the standard CDM picture, the density perturbation is generated primordially by the Gaussian vacuum fluctuation when the universe resides in the inflationary phase. In this picture, small scale fluctuations are generated through the previously mentioned Sachs-Wolfe effect (Sachs & Wolfe 1967) and the Doppler effect of hot electrons (Gorski 1992) at the last scattering surface. The velocity dispersion of hot electrons obeys Boltzman statistics; thus, the temperature fluctuation is Gaussian regardless of the nature of the perturbation. For the Sachs-Wolfe effect, the temperature fluctuation is related to the gravitational potential at the last scattering surface. Since the potential is a sum over all density waves of the perturbation, the central limit theorem guarantees that the temperature will be Gaussian, even if the underlying density perturbation is highly non-Gaussian (Scherrer & Schaefer 1992). Thus, in the standard picture, the temperature fluctuations are always Gaussian.

In the COBE experiment, when convolving with a 10° FWHM beam, the non-Gaussian characteristic features are essentially lost. However, small scale experiments can still provide us information about the nature of the perturbations, and, in turn, test models of structure formation.

Until the present, the UCSB South Pole data have been analyzed by assuming a Gaussian distribution signal on the sky,

$$P(\Delta) = (2\pi\sigma_\Delta)^{-1} \exp(-\Delta^2/2\sigma_\Delta^2), \quad (5.1)$$

and, if the signals are coming from the cosmic microwave background radiation (CBR), they are correlated and characterized by a common autocorrelation function:

$$C(\theta) = C(\hat{m} \cdot \hat{n}) = \left\langle \frac{\Delta T}{T}(\hat{m}) \frac{\Delta T}{T}(\hat{n}) \right\rangle. \quad (5.2)$$

The 95% confidence level (C.L.) limits quoted in the paper were derived by assuming a Gaussian autocorrelation function:

$$C(\theta) = C_0 \exp\left(-\frac{\theta^2}{\theta_c^2}\right), \quad (5.3)$$

where $C_0 = \sigma_\Delta^2 = \int_0^\infty P(\Delta)\Delta^2 d\Delta$ is the rms temperature anisotropy.

The Gaussian correlation in Eq.(3) is a convenient way to present results rather than an a priori assumption in the analysis. The autocorrelation is exactly calculable. For example, in the inflationary paradigm, it is given by the Holtzman (1989) correlation function; the autocorrelation function for planar domain walls and sub-horizon vacuum bubbles are also available (Luo & Schramm 1993). But it becomes very complicated to do the Bayesian analysis of the data, especially when the distribution function is non-Gaussian. Therefore, we first perform a robustness test of the Gaussian correlation function in Eq. (3) by asking the following question: if the data are uncorrelated, how do the results change relative to the results from analysis of correlated data? If Eq.(3) is a fairly robust assumption, in the non-Gaussian case, we can treat the data as statistically independent.

The likelihood function for N statistical independent data is (Eadie et al. 1971):

$$L(C_0, \sigma) = \prod_{i=1}^N f(C_0, \sigma_i), \quad (5.4)$$

where f is the common probability distribution function. The likelihood function for 4 different channels of the UCSB South Pole data is shown in Fig. (7) when f takes the Gaussian form given by Eq.(5.1). As shown in Fig. (8), the 95% confidence level limits on ΔT calculated from the high frequency channel is $29.7 \mu K$, or $\frac{\Delta T}{T} < 1.1 \times 10^{-5}$, which is slightly stronger than the limits from correlated data.

If a value for $\Delta T/T$ much below 1.4×10^{-5} is eventually confirmed, it would be difficult for any Gaussian model to fit the observed large scale velocity flows and also the extra power reported by the APM survey, one may be forced to introduce the idea of early reionization of the universe to resolve the puzzle and retain a Gaussian picture. However, the new 15 point experiment (Gundersen 1992) doesn't seem to be as restrictive as the previous 9 point experiment so care needs to be taken here to discuss reionization. In this paper, we don't consider reionization and the present analysis is clearly preliminary.

Now, let us focus our attention on the Gaussian assumption of temperature fluctuations given by Eq. (5.1). A number of non-Gaussian probability distribution functions can be tested through the original nine available data points (Gaier et al. 1992). Since the functional space of a non-Gaussian distribution is infinite, one has to choose some statistical measures to quantify the discussion. Among them, skewness and kurtosis, which are the third and fourth moments of the distribution function (Luo & Schramm 1992), are often used. Skewness S shows the non-symmetric deviation from a Gaussian. If $S \neq 0$, there will be excessive fluctuations at the hot (or cold, depending on $S > 0$ or not) end. Kurtosis K is more interesting in that it shows a symmetric deviation from Gaussian. As we noted in a previous paper on the cosmological density field (Luo & Schramm 1992b), it will be very interesting if a negative kurtosis is discovered. For the temperature fluctuation of CBR, this is especially true since negative kurtosis can be associated with hot (or cold) spots on the CBR sky which are predicted by several models of structure formation. In the ideal case when there is only one hot and one cold in the sampling region, the distribution function will be:

$$f(x) = 1/2(\delta(x - A) + \delta(x + A)), \quad (5.5)$$

which has a kurtosis of $K = -2 < 0$. When there are a number of hot and cold spots in one sampling area, we can use the following distribution function:

$$f(x, \mu, \sigma) = \frac{1}{2\sqrt{2\pi}\sigma} \left\{ \exp\left(-\frac{(x - \mu)^2}{2\sigma^2}\right) + \exp\left(-\frac{(x + \mu)^2}{2\sigma^2}\right) \right\}, \quad (5.6)$$

which is the sum over two Gaussians, centered at $\pm\mu$ respectively, which corresponds to separated hot and cold regimes. μ is related to the averaged amplitude of the hot and cold spots and the width of the Gaussian, σ , is related to the angular size of the spots. If we assume that all spots have the same amplitude and that there are an equal number of cold and hot spots in the sampling area, then the parameters (μ, σ) in Eq. (5.6) are related to the physical parameters of the hot and cold spots (\bar{A}, N) through:

$$\begin{aligned} \mu &\sim \frac{1}{N}\bar{A}, \\ \sigma &\sim \frac{N-1}{N}\bar{A}, \end{aligned} \quad (5.7)$$

where \bar{A} is the amplitude of a spot and N is the number of hot (or cold) spot. In the limit $N = 1$, $\sigma \rightarrow 0$, $\exp\left(-\frac{(x \pm \mu)^2}{2\sigma^2}\right) \rightarrow \delta(x \pm \mu)$, thus $f(x) \rightarrow 1/2(\delta(x + A) + \delta(x - A))$, which recovers the result of Eq. (5.5).

The variance (rms temperature fluctuation) and the kurtosis of the distribution given in Eq. (5.6) are:

$$\left(\frac{\Delta T}{T}\right)_{rms}^2 = \bar{x}^2 = \mu^2 + \sigma^2, \quad (5.9)$$

$$K = \frac{\bar{x}^4}{(\bar{x}^2)^2} - 3 = -2 \frac{\mu^4}{(\mu^2 + \sigma^2)^2}. \quad (5.10)$$

In Fig. 9, we plot the distribution given by Eq. (5.8) with $\sigma = 1$ and kurtosis $K = -0.5$. The kurtosis is negative whenever there are spots in the CBR temperature distribution. Thus, a measurement of kurtosis, K , provides a quantitative way to hunt for possible existing hot and cold spots on the CBR sky.

The results are summarized in Fig. 10a, 10b. The present observational limits from Gaier et al. have already placed very strong limits on the possible existence of hot and cold spots on the CBR sky. Analyzing the data by assuming that the signals are uncorrelated (full analysis by taking into account the correlation will be presented later), the observations rule out any spot of angular size of $\sim 1^\circ$ with amplitude of $28 \mu K$ at the 95 % C.L. which suggests that the amplitude of the temperature fluctuation $\delta T/T \lesssim 1.05 \times 10^{-5}$ at 1° scale. Implications for different non-Gaussian models are the following:

(1) Cosmic texture. The amplitude of temperature fluctuations for cosmic texture (Turok & Spergel 1991) is

$$\delta T/T \sim 8\pi^2 G\eta^2$$

which is independent of the angular size. From the limits where

$$(\delta T/T)_{spot} \lesssim 1.05 \times 10^{-5}$$

we have

$$G\eta^2 = (\phi_0/M_p)^2 \lesssim 2 \times 10^{-7}$$

which tightly constrains cosmic texture as a candidate for structure formation.

(2) Domain wall bubbles. The characteristic amplitude of a collapsing vacuum bubble (Turner, Watkins, & Widrow 1991) is

$$\delta T/T = 2.64 \times 10^{-4} \beta \left(\frac{\sigma}{10 \text{MeV}^3} \right) A$$

where (β, \tilde{A}) are the numerical constant of order unity. Thus the constraint on $\delta T/T$ shows that the surface tension of the wall will be

$$\frac{\sigma}{10\text{MeV}^3} \lesssim 5 \times 10^{-2}, \quad \sigma < 0.5\text{MeV}^3.$$

Domain walls with this surface tension are too light to directly form any cosmologically interesting structure. This result probably eliminates domain wall bubbles as candidates for accreting sites that form small scale structure unless some new exotic physical process is involved to stabilize the bubble. Large domain walls interacting with matter (Massarotti 1991) or the mixtures of strings and walls (Luo & Schramm 1992c) may still be viable models.

(3) Cosmic strings. As shown by Bouchet, Bennett, & Stebbins (1988), the CBR anisotropies are non-Gaussian on arcminute scales or smaller. They tend to be Gaussian on the scales probed by COBE, balloon experiments and South Pole experiments. Thus, the current bound doesn't constrain the cosmic string models at all. So far, it is the most successful viable non-Gaussian alternative to generate cosmic structure. Cosmic strings can be generated in LTPT as well as in primordial transitions. However, in LTPT, the strings can be thick (Luo & Schramm 1992c) and some aspects of the traditional string analysis (Bouchet et al. 1988) may not apply.

(6) Surviving Models and Observational Tests

In summary, there are three viable LTPT models which satisfy the current observational tests:

- (1) HDM with LTPT models
- (2) Open universe with $\Omega_m = 0.2$ and LTPT.
- (3) Cosmological constant dominated universe with LTPT.

While we personally favor (1) for the reason of "naturalness", at present, (2) and (3) are also still allowed by actual observations. The unique observational tests for LTPT includes the following

(1) The observation of temperature fluctuation on arcmin scale or smaller. In the primordial cases, the finite thickness of the last scattering surface washes away all the anisotropy on scale less than ~ 8 arcmin. However, if the perturbations are generated via

LTPT, the anisotropies persist. Thus, a detection of CBR fluctuations on scales less than 8 arcmin at the level of 10^{-5} will provide convincing evidence for LTPT.

(2) The mass of the neutrino. The MSW mechanism invoked to solve the solar neutrino problem suggests massive neutrino and neutrino flavor mixing. The τ -neutrino mass implied by the see-saw mechanism could be around 30 eV, which provides the closure mass density of the universe. If future experiments detect the neutrino mass and confirm that the dark matter in the universe is hot, model (1) will be an attractive model.

(3) Detection of the break of the power spectrum at the scale $\sim 1000\text{Mpc}$. As we showed in Fig. 4, the power spectrum of model (2) and (3) has a break around $\lambda_d \sim 1000\text{Mpc}$. The power spectra index changes from $n \sim 1$ to $n \sim 4$. This length scale corresponds to the horizon size of the universe when the universe becomes curvature or vacuum dominated. Thus an analysis of the break of the power spectrum provides a decisive test of the model (2) and (3).

(4) Proof of non-Gaussianity by a non-zero kurtosis (Luo & Schramm 1992c) or by the three point temperature correlation function (Luo & Schramm 1993) would establish the need for topological defects. Many defects are optimally viable in LTPT.

The LTPT models bear the hope that the cosmic structure can be explained by some causal physical process rather than invoking new, fundamental physics. In this paper, we presented the relatively model independent result for structure formation via LTPT and discuss the possible viable models after taking into account the current observational constraints. If future experiments decisively kill the LTPT model, it will imply that the seeds (fluctuations) are indeed primordial, thus provides another solid evidence that important new physics beyond $SU(3) \times SU(2) \times U(1)$ is required for cosmic structure formation.

Acknowledgements

We want to thank Michael Turner, Josh Frieman, Stephan Meyer, Albert Stebbins and Andrew Jaffe for useful discussion. This work is supported in part by NSF grant #90-22629 and by NASA grant #NAGW 1321 at the University of Chicago and by the DOE and by NASA through grant #NAGW 2381 at Fermilab.

REFERENCES

- Bahcall, N. 1992, Princeton POP-490, to appear in Proc. of N.A.S. Colloquium on Physical Cosmology, Irvine, Cal. March 1992, ed. D.N. Schramm (Washington, DC: Proc. Nat. Acad. Sci), in press
- Bardeen, J.M., Steinhardt, P.J., & Turner, M.S. 1983, Phys. Rev. D, 28, 679
- Bennett, C. et al. 1992, ApJ, 396, L7
- Bouchet, F.R., Bennett, D., & Stebbins, A.J. 1988, Nature, 335, 410
- Carrol, S., Press, W., & Turner, E. 1992, Ann. Rev. Astron. and Astrophys., 30 499
- Davis, M., & Peebles, P.J.E. 1983, ApJ, 267, 465
- Davis, M., Summers, F.J., & Schlegel, D. 1992, Nature, 359, 393
- Dressler, A. et al. 1987, ApJ, 313, L37
- Eadie, W.T., Drijard, D., James, F.E. & Sadoulet, B. 1971, Statistical Methods in Experimental Physics (North Holland, 1971)
- Freese, K., Frieman, J., & Olinto, A. 1990, Phys. Rev. Letters, 65, 3233
- Gaier, et al. 1992, ApJ, 399, L1
- Geller, M. & Huchra, J. 1989, Science, 246, 897
- Gorski, K. 1992, ApJ, 398, L5
- Gouda, N., Sasaki, M., & Suto, Y. 1989, ApJ, 341, 557
- Gundersen, J. 1992, talk given at APS meeting in Fermilab.
- Guth, A.H. & Pi, S.Y., Phys. Rev. Letters, 49, 1110 (1982)
- Hawking, S.W. 1982, Phys. Letters B, 115, 295
- Hill, C., Schramm, D.N. & Fry, J. 1989, Comments on Nucl. Part. Phys., 19, 25
- Hill, C.T., Schramm, D.N., & Widrow, L. 1990, in Particle Astrophysics: The Early Universe and Cosmic Structures, ed. J.M. Alimi et al. (Gif-sur-Yvette: Editions Frontières), 315
- Jaffe, A., Stebbins, A., & Frieman, J. 1992, Fermilab-Pub-92/362-A

Kashlinsky, A. 1992, ApJ, 399, L1
Kashlinsky, A. 1992, ApJ, in press
Klemperer, W., Luo, X.C., Rosner, R., & Schramm, D.N. 1992, Fermilab-Pub-92/38-A
Kolb, E. & Turner, M.S. 1990, The Early Universe (Redwood City: Addison Wesley)
Luo, X.C., Schramm, D.N. 1992a, Science, 256, 513
Luo, X.C., Schramm, D.N. 1992b, ApJ, in press
Luo, X.C., Schramm, D.N. 1992c, ApJ, 394, 12
Luo, X.C., Schramm, D.N. 1993, ApJ, submitted
Massarotti, A. 1991, Phys. Rev. D, 43, 346
Meyer, S. et al. 1991, ApJ, 317, L7
Ganga et al. 1993, ApJ, submitted
Press, W., Ryden, B., & Spergel, D. 1990, Phys. Rev. Letters, 64, 1084
Peacock, J. 1991, MNRAS, 253, 1p
Schaefer, R.K. & Shafi, Q., Nature, 359, 199
Scherrer, R. & Schaefer, R. 1992, OSU preprint
Silk, J. 1967, Nature, 215, 1155
Smoot, G. et al. 1992, ApJ, 396, L1
Starobinskii, A.A. 1982, Phys. Letters B, 117, 175
Turok, N. & Spergel, D. 1991, Phys. Rev. Letters, 66, 3093
Weinberg, S. 1972, Gravitation and Cosmology (John Wiley & Sons, Inc.)
Wilson, M.L., & Silk, J. 1981, ApJ, 243, 14
Wright, E. et al. 1992, ApJ, 396, L13

FIGURE CAPTIONS

Fig. 1: For three different cases, the comoving horizon size λ as a function of the scale factor R .

Fig 2: δ vs scale factor R .

Fig. 3: Power spectrum in LTPT models. The standard CDM and HDM power spectrum are also plotted in the graph for comparison.

Fig. 4: The power spectrum for LTPT models when the universe is either vacuum or curvature dominated.

Fig. 5: Power spectrum of density perturbation in HDM with LTPT models.

Fig. 6: The angular two point function $\omega(\theta)$ predicted from the HDM with LTPT models. Note the agreement with the APM data.

Fig. 7: The likelihood function of 4 different channels for South Pole data set. The three low frequency channels all show the detection of a signal. But the trend that, as the frequency gets higher, the position of maximum likelihood shifts to the lower end of ΔT , is probably a signature of low frequency background contamination.

Fig. 8: 95% C.L limits to ΔT . The black squares are the limits to which the data are correlated. The diamonds are limits from uncorrelated data. Note that the limits from uncorrelated data are stronger.

Fig. 9: Distribution function given by Eq. (5.8) with kurtosis $K = -0.5$. The dotted line is a Gaussian with the same variance.

Fig. 10a: The likelihood as a function of the size and amplitude of the hot and cold spots on CBR sky.

Fig. 10b: 95% C.L. on $\frac{\delta T}{T}$ as a function of the kurtosis of the distribution.

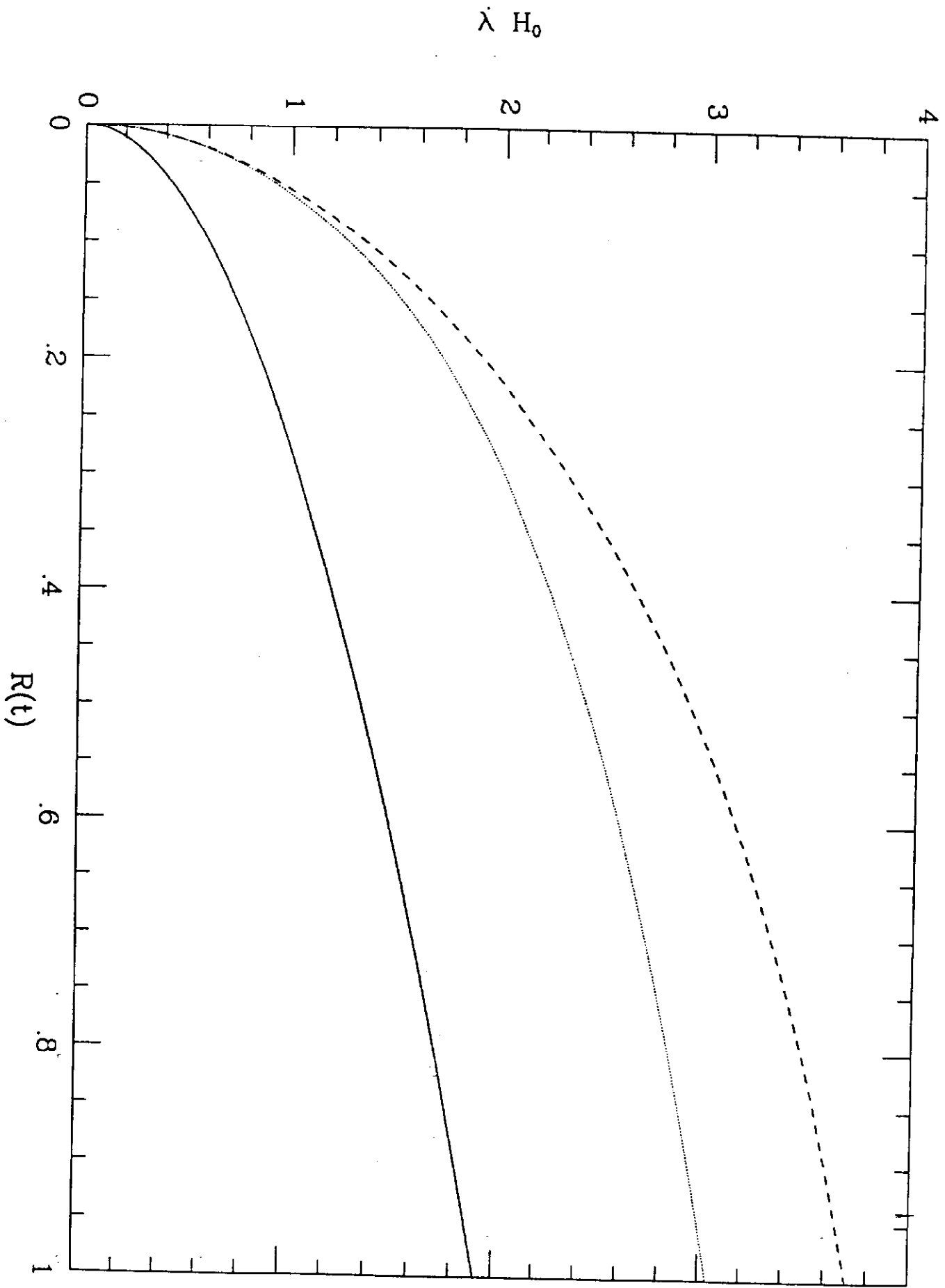


Fig. 1

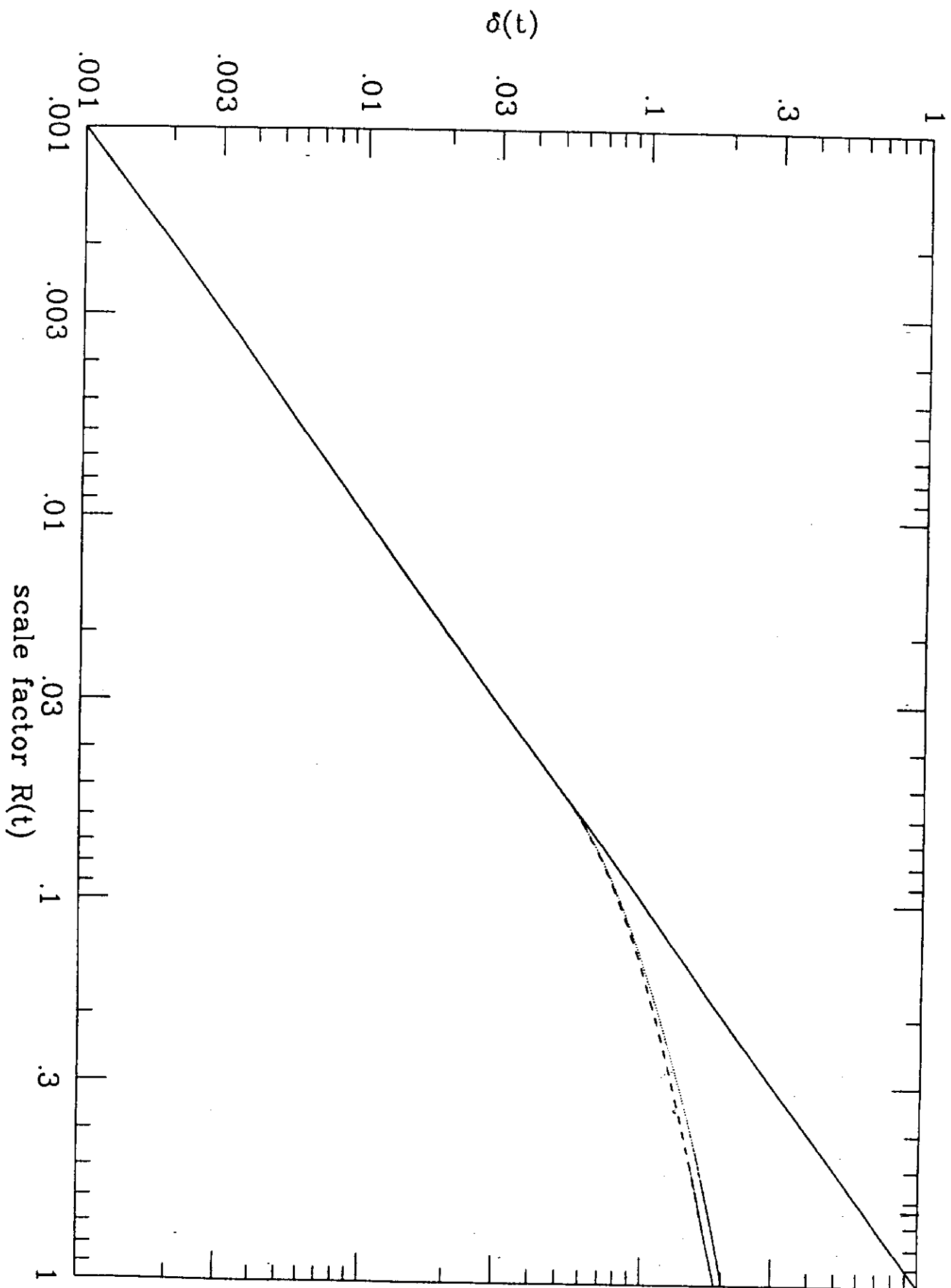


FIG 2

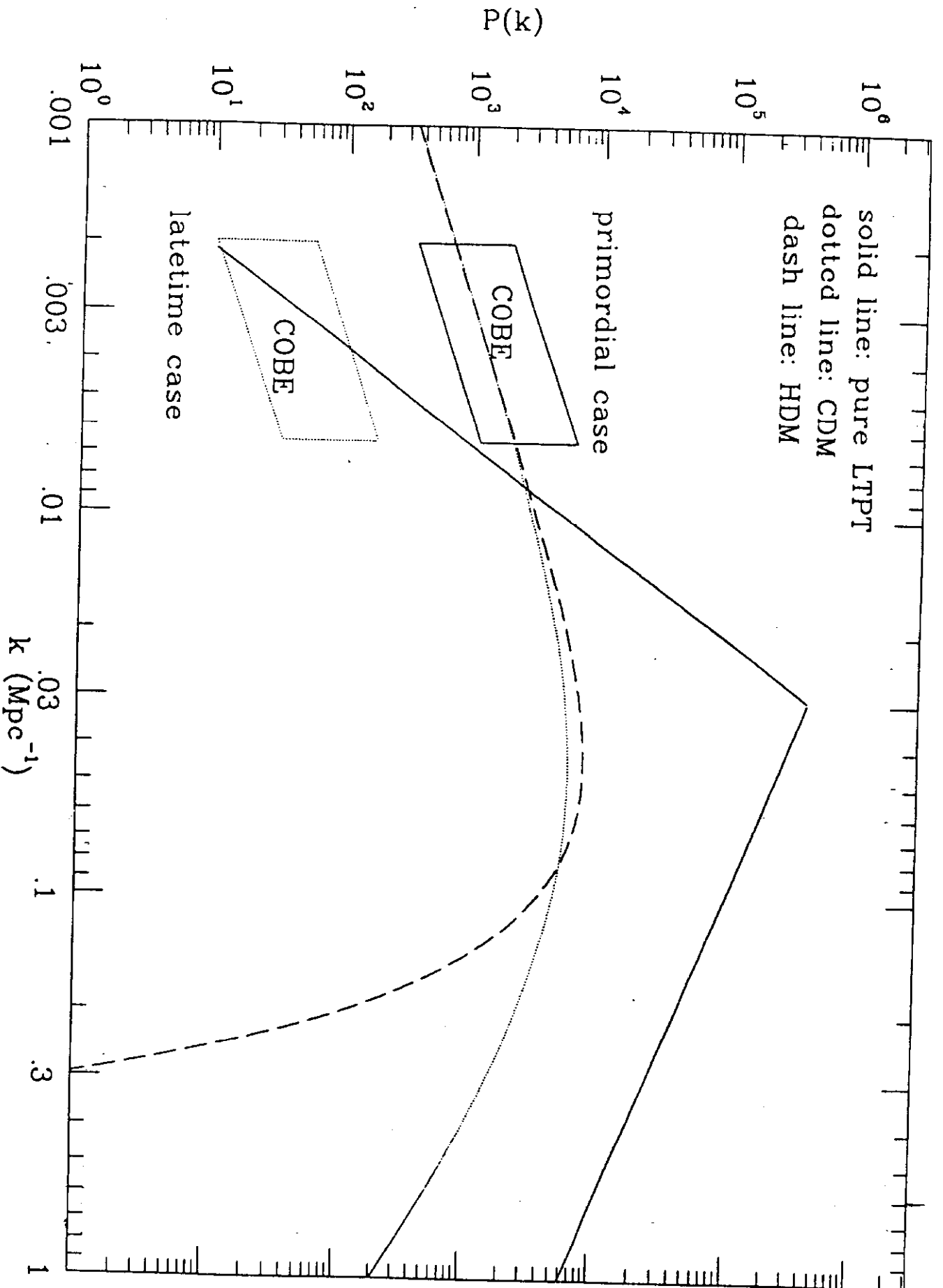


Fig 3

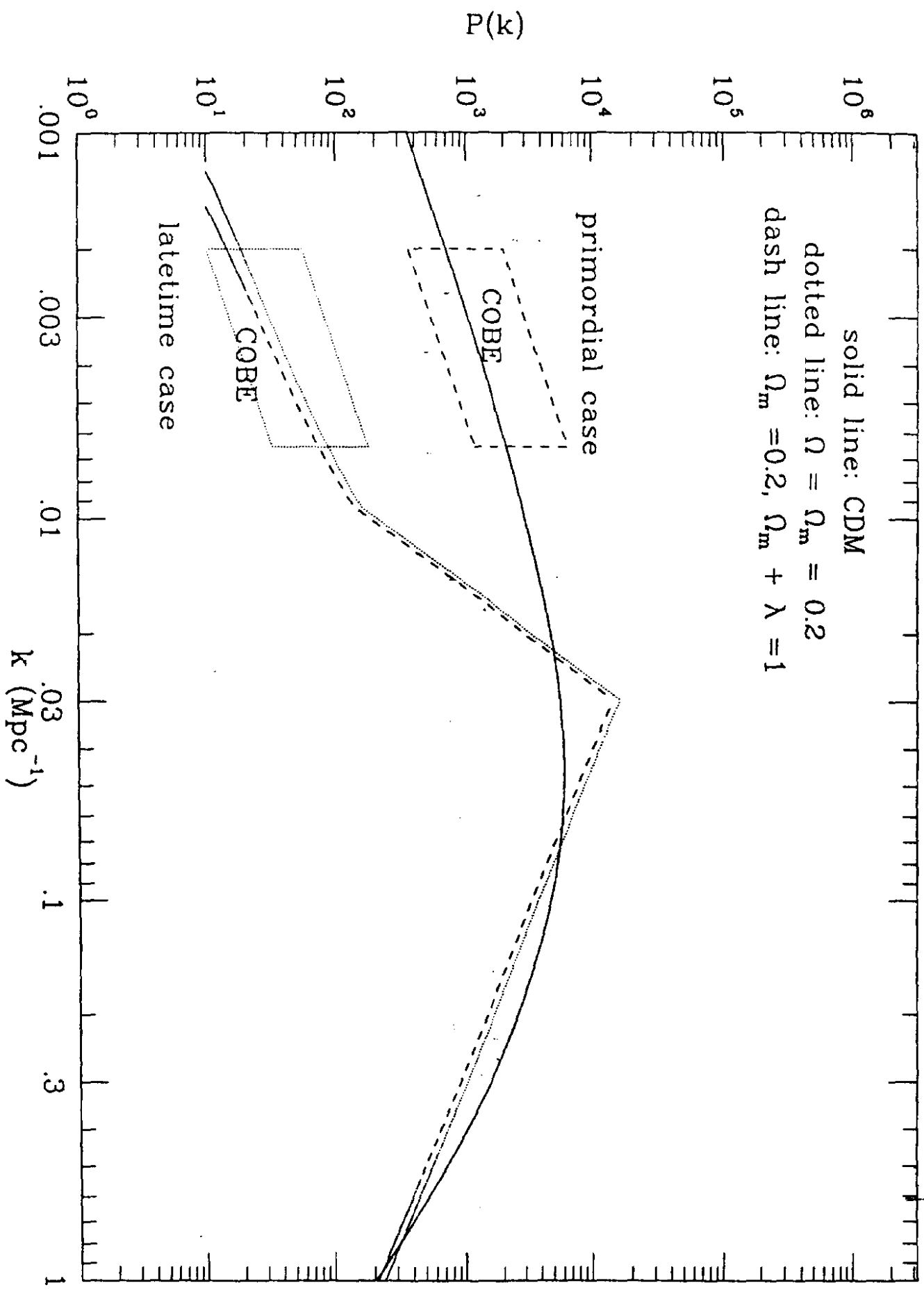


Fig 4

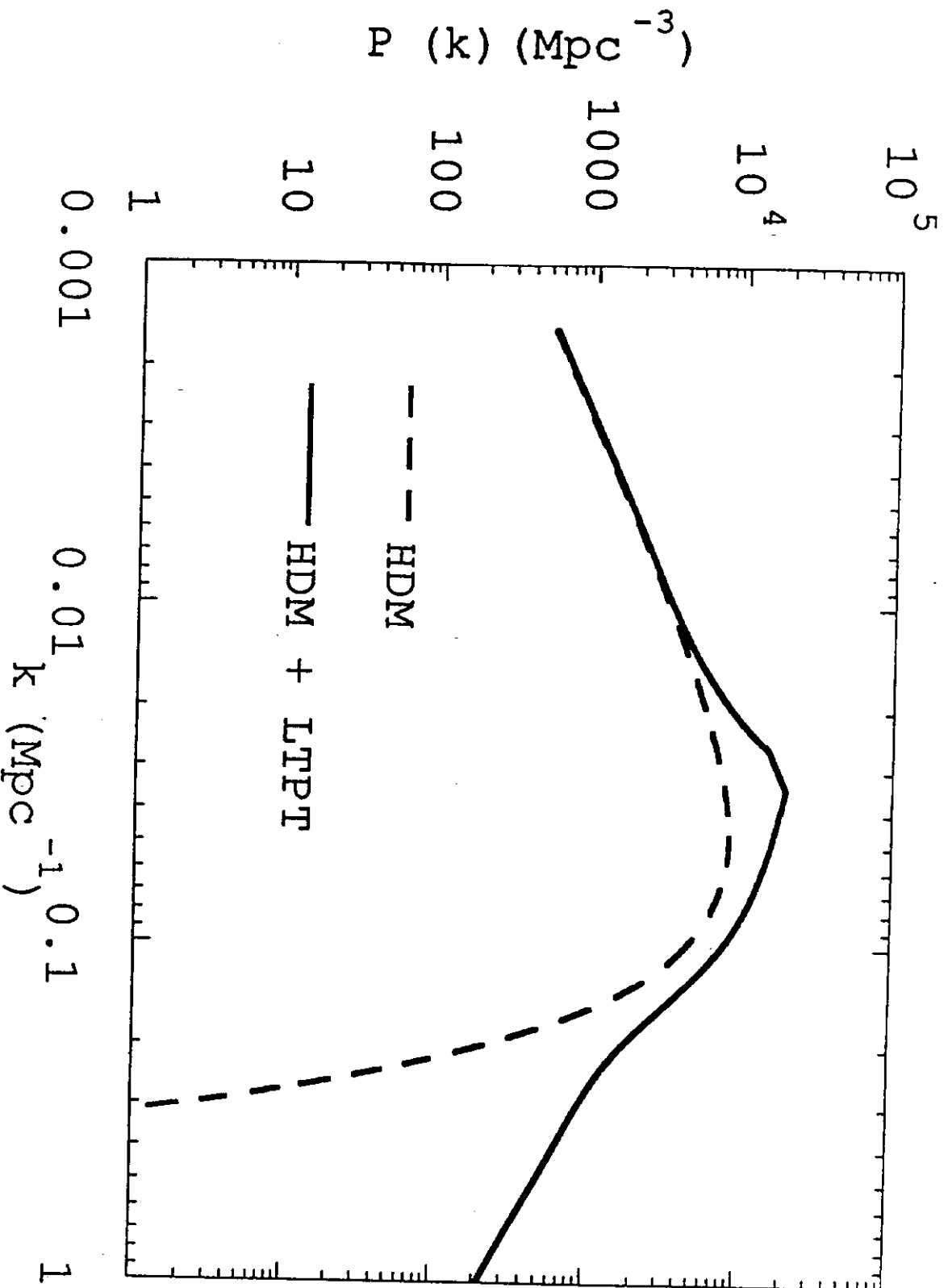


Fig 5

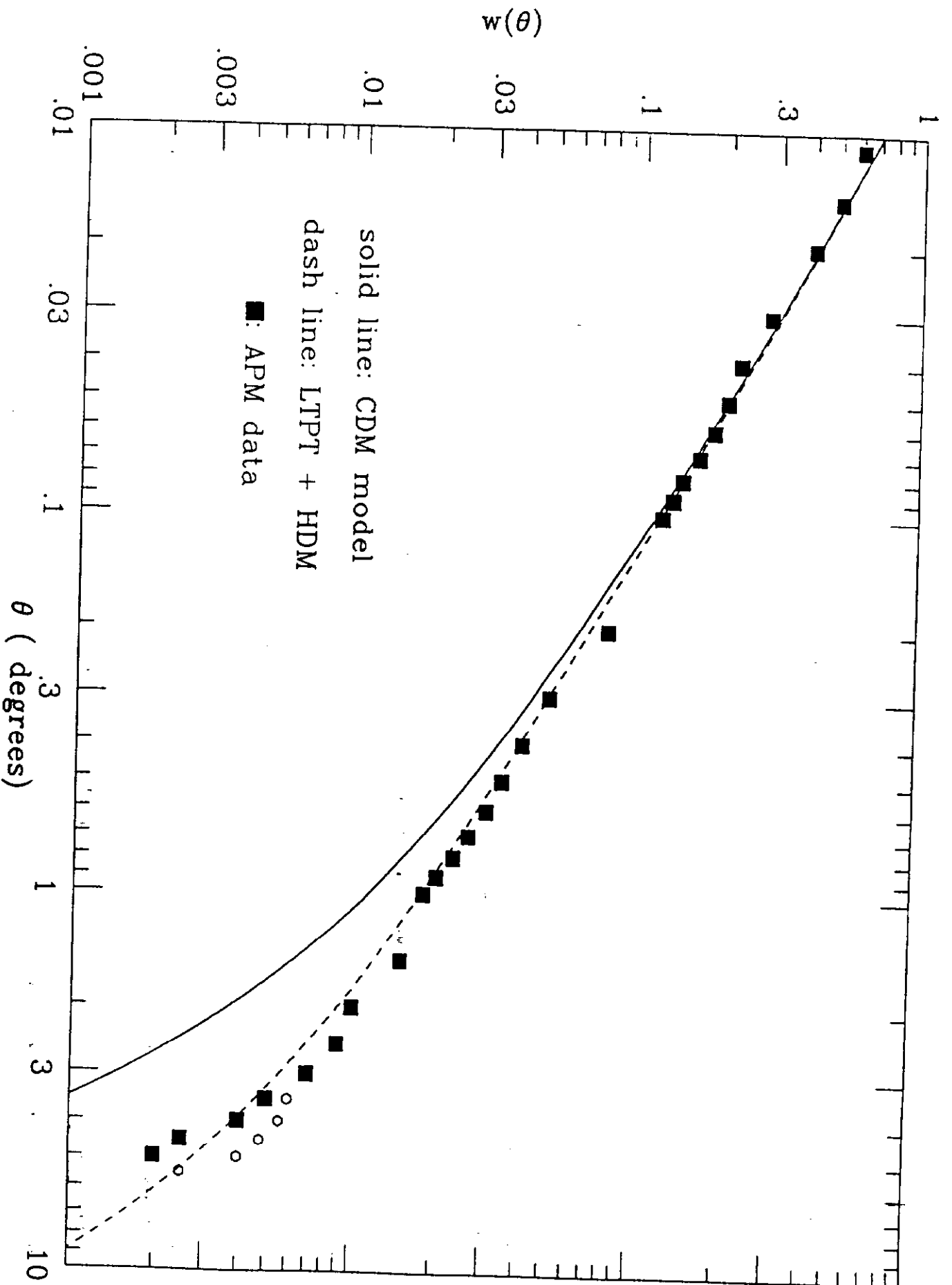


Fig. 6

likelihood function

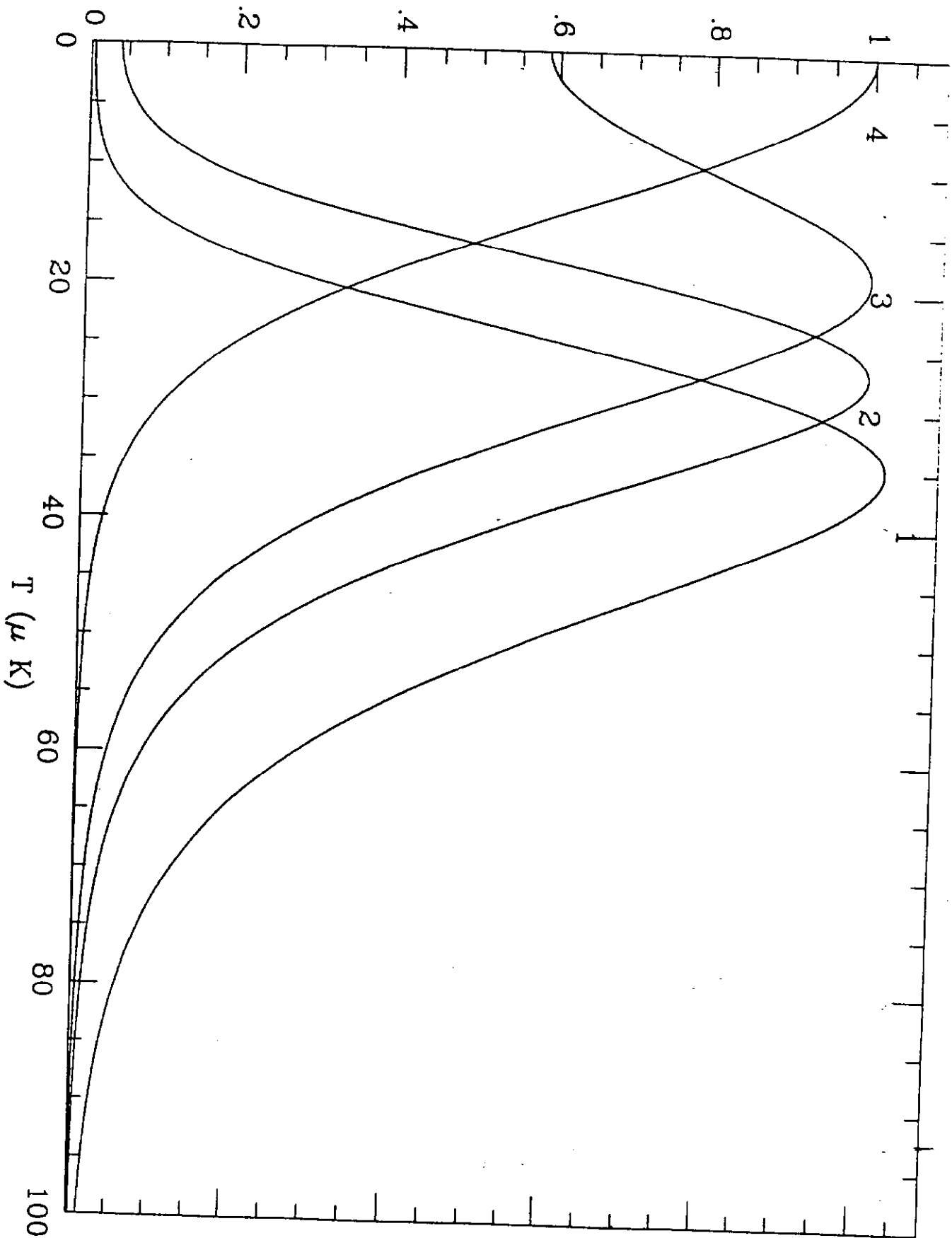


Fig 7

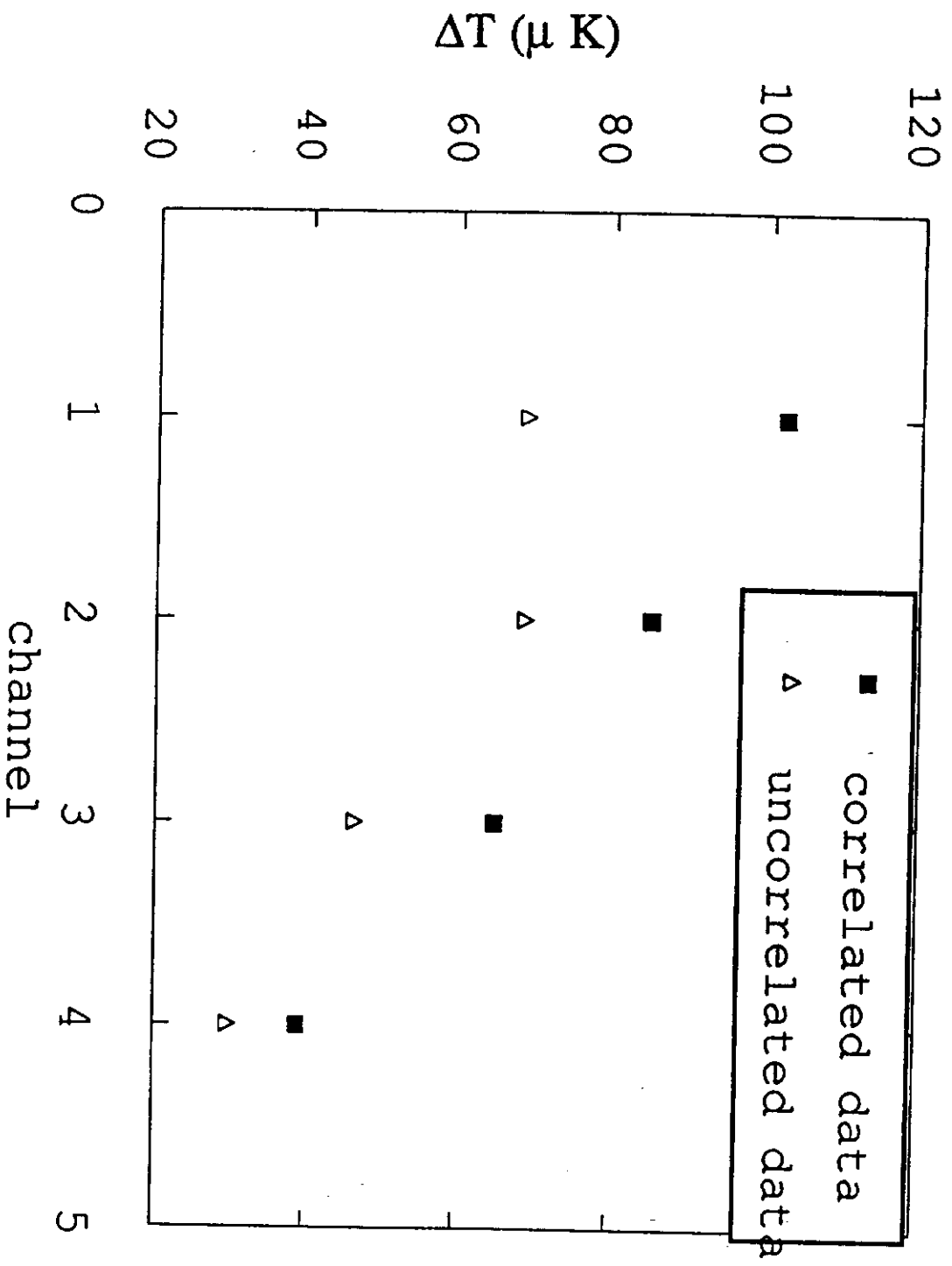


Fig 8

$f(x)$ (kurtosis $K = -0.50$)

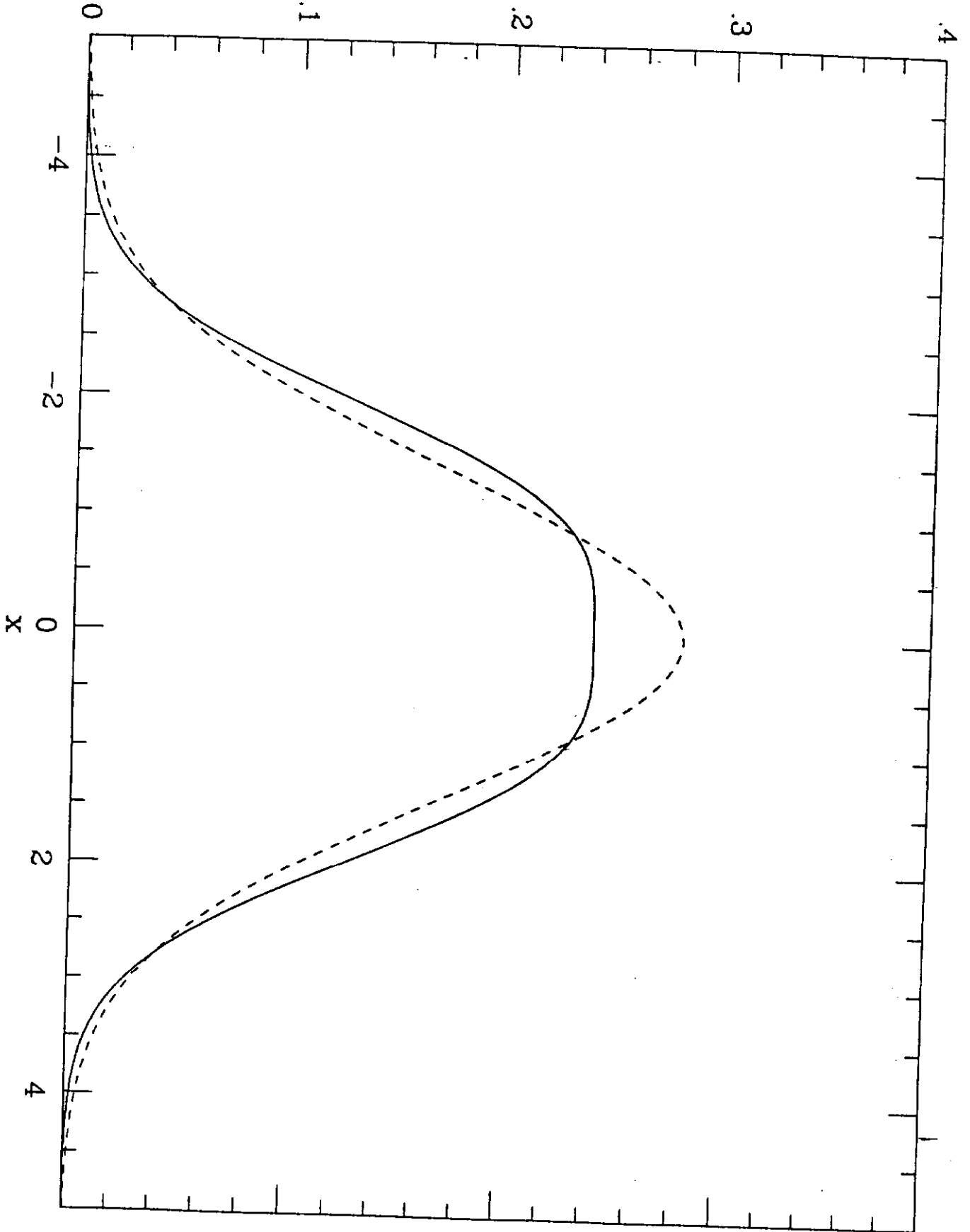


Fig 9

Likelihood function

"galerl.data"

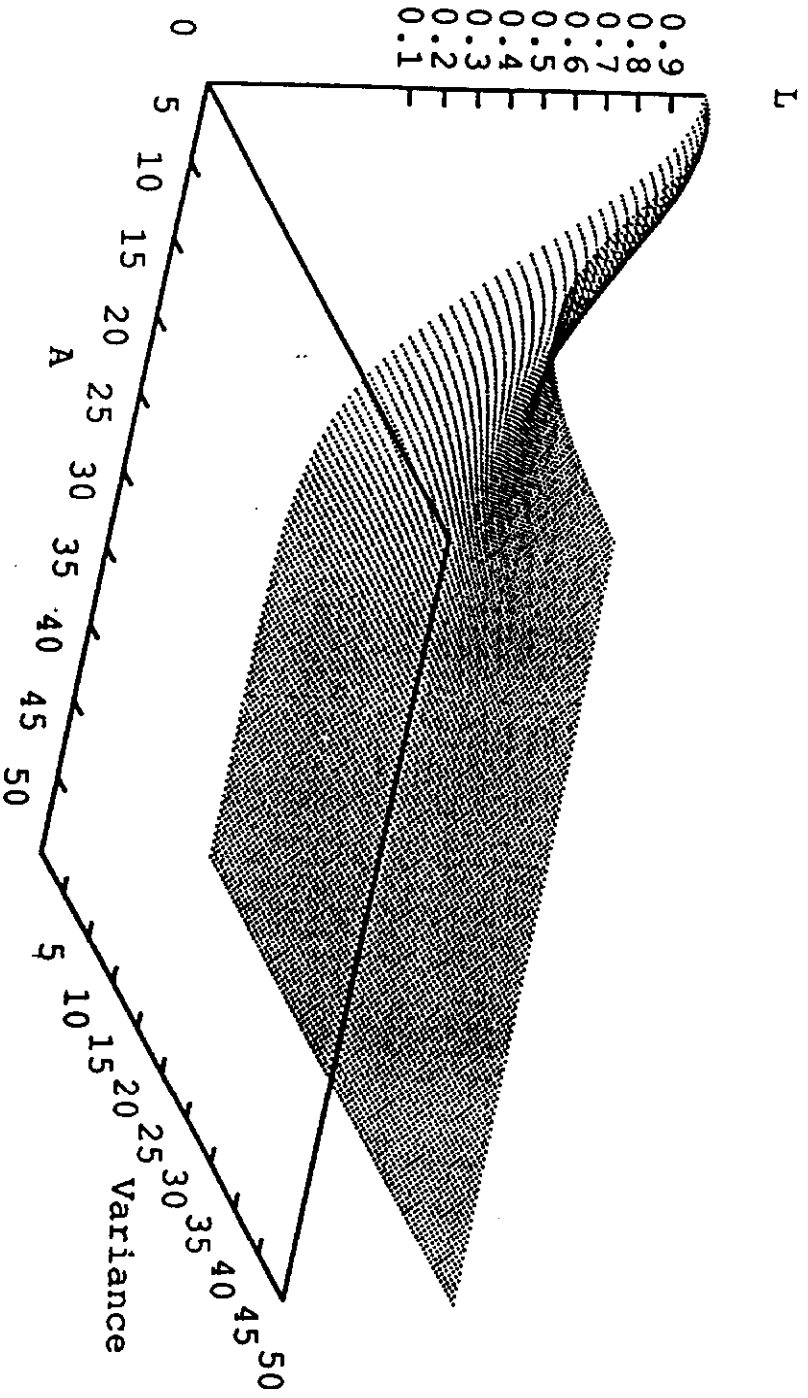


Fig 10a

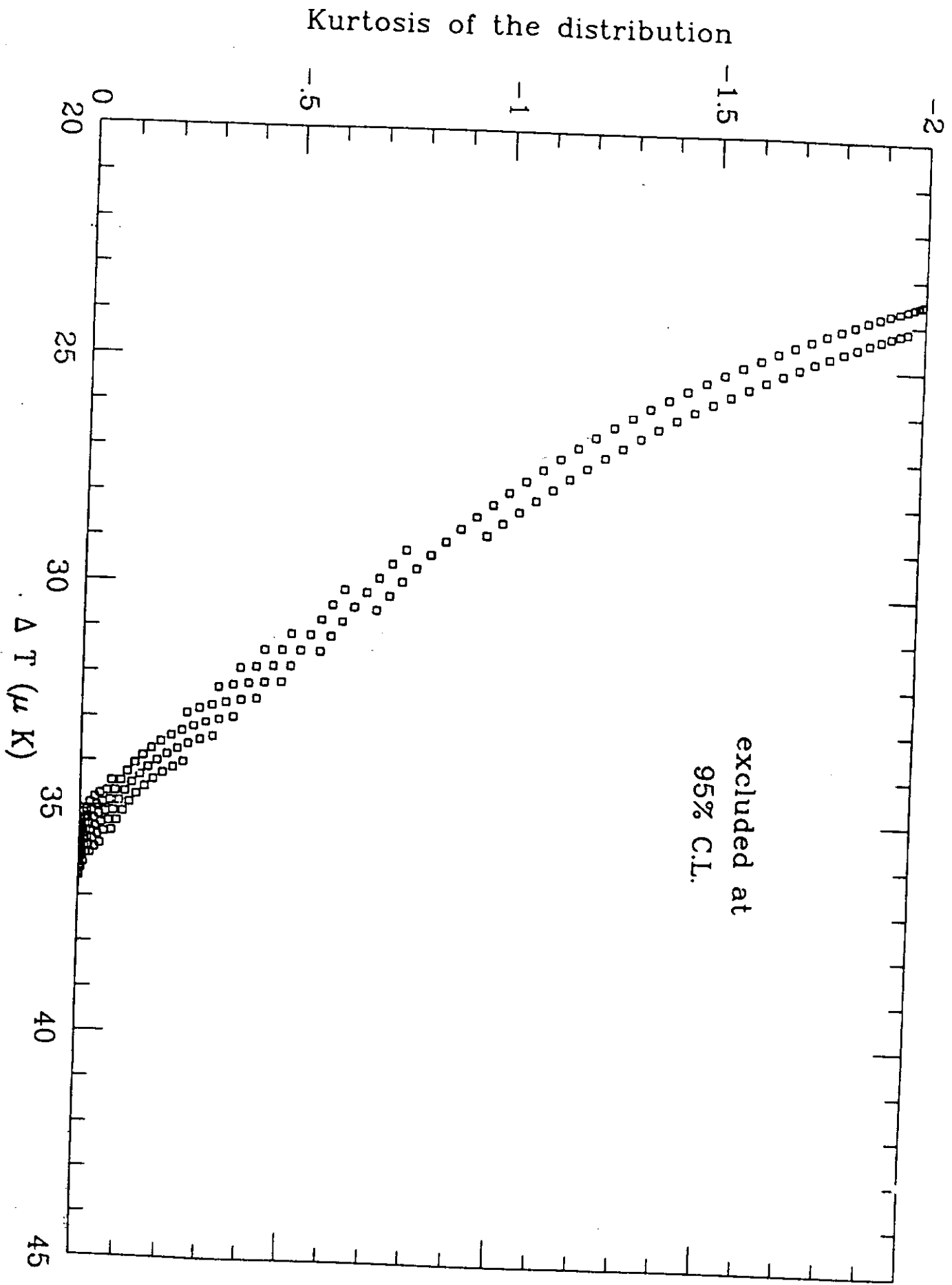


Fig. 106